Eurographics Symposium on Rendering 2017
P. Sander and M. Zwicker
(Guest Editors)

Volume 36 (2017), Number 4

Supplemental Material for Line Integration for Rendering Heterogeneous Emissive Volumes

Florian Simon[1,2†] Johannes Hanika[1,2] Tobias Zirr[1] Carsten Dachsbacher[1]

[1]Karlsruhe Institute of Technology [2]Weta Digital Ltd.

1. Additional Proof of the Track Length Estimator

In the following we will give an alternative way to show that the track length estimator

$$\frac{1}{N}\sum_{i=1}^{N}\int_0^{t_i} \text{Ł}_e(s)\,ds,$$

where t_i is sampled proportional to transmittance, is an estimator for

$$\int_0^{\infty} \text{Ł}_e(t)\tau(t)\,dt$$

First, we define a probabilistic estimator for the transmittance using a random distance s with $p(s) \propto \tau(s)$ as

$$\tau'_s(t) = \begin{cases} 1, & \text{if } t \leq s \\ 0, & \text{otherwise.} \end{cases}$$

This estimator is unbiased because

$$\mathbb{E}\left[\tau'_s(t)\right] = \int_0^{\infty} \tau'_s(t)p(s)\,ds = \int_t^{\infty} p(s)\,ds = \tau(t)$$

and since the distances of the track length estimator are sampled proportional to transmittance we can write

$$\begin{aligned} \mathbb{E}\left[\int_0^{t_i} \text{Ł}_e(t)\,dt\right] &= \mathbb{E}\left[\int_0^{\infty} \text{Ł}_e(t)\,\tau'_{t_i}(t)\,dt\right] \\ &= \int_0^{\infty} \text{Ł}_e(t)\,\mathbb{E}\left[\tau'_{t_i}(t)\right]\,dt \\ &= \int_0^{\infty} \text{Ł}_e(t)\,\tau(t)\,dt. \end{aligned}$$

Note that this is only a special case of our line estimator and does not work for different distance sampling for t_i, for example equi-angular sampling. Our approach with weight functions is more general and independent of the distance sampling method.

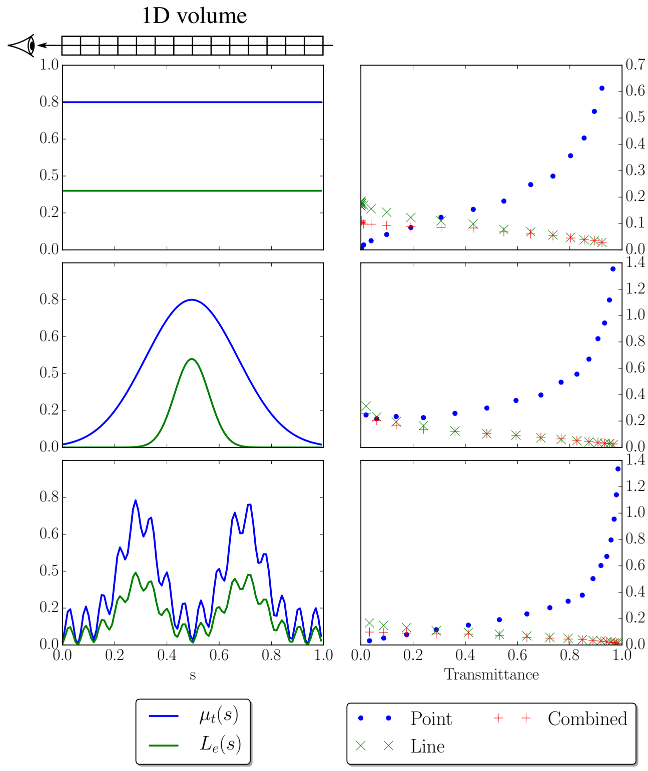

Figure 1: *The functions $\mu_t(s)$ and $L_e(s)$ shown in the left columns are rasterized into a 1D volume (100 voxels). The point, line, and combined estimators are evaluated with 32 samples for multiple density scales. The plots on the right show the RMSE of all estimators depending on the transmittance through the whole volume.*

2. Addional Results

To evaluate the different estimators (point, line and combined) we tested three simple 1D volumes and numerically computed the incident radiance by integrating the volumetric emission along a ray as seen in Fig. 1. The rows of the plot correspond to different volumes where μ_t and L_e are shown in the left column. We performed this experiment for varying σ_t and plotted the root-mean-squared error (RMSE) to a reference solution after 32 samples depending on the total transmittance of the volume. For normalization we chose σ_e such that the total incident radiance is one.

From the plots we can see that the line and combined estimators gain advantage over the traditional point estimator increasing transmittance. However, for very dense volumes the point estimator is better than the line estimator since the segment length introduces additional variance. The combined estimator performs better than the line estimator in this case, although it does not reach the quality of the point estimator for dense volumes. We provide the code with which these plots where generated, containing simple implementations for the estimators, as a Python script.

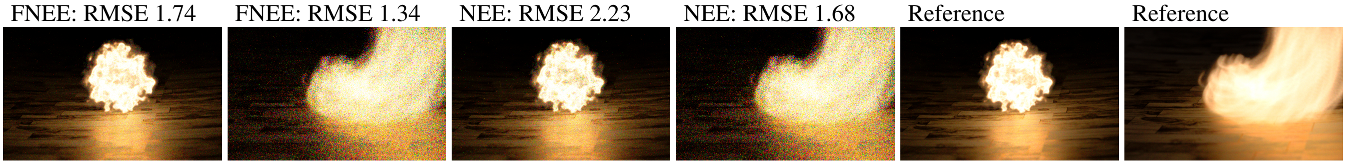

Figure 2: *A non-linear motion blur test case to demonstrate compatibility of our method with requirements of contemporary rendering systems. The images are equal-sample (64 spp) and the medium parameters are $\sigma_t = 1.0$, $\sigma_s = 0.2$, $\sigma_e = 0.5$. Here, FNEE took 12% longer to render the image compared to NEE (31% in the static case).*

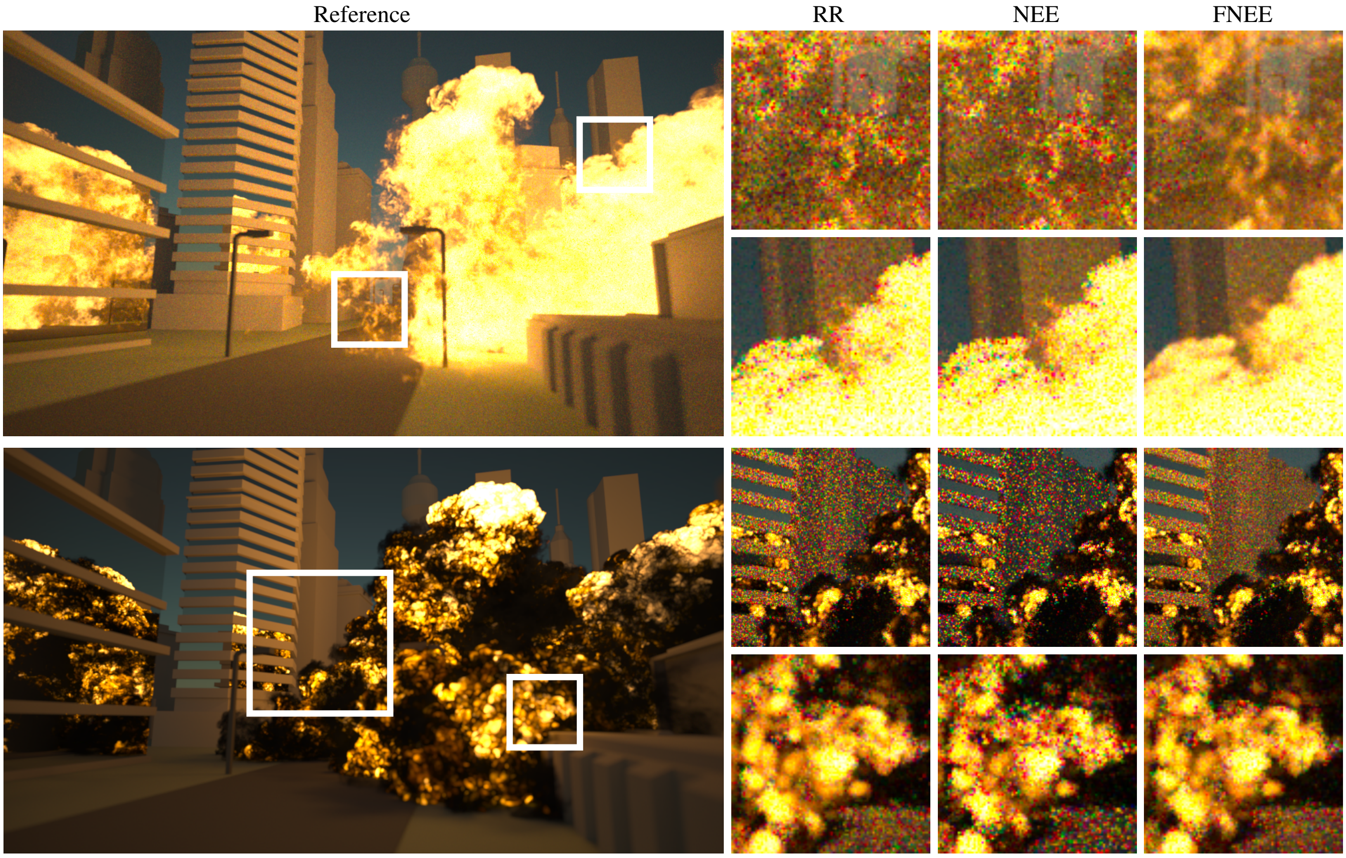

Figure 3: *Equal-time comparison of the NEE with probabilistic transmittance sampling (RR), regular NEE (NEE) and our FNEE. In the thin version (top row), RR has the same quality as NEE whereas in the dense version (bottom row) the larger sample count of RR leads to an improvement compared to NEE. FNEE outperformes RR and NEE in both cases.*

In Fig. 2 we show that our technique is also beneficial in scenes with motion blur.

Fig. 4 shows larger images of the scalability test using a 30GB volume.

Probabilistic Transmittance for NEE Fig. 3 shows an equal-time comparison of the NEE with probabilistic transmittance sampling (RR), regular NEE (NEE) and our FNEE. In the thin version (top row, 10min), RR has the same quality as NEE whereas in the dense version (bottom row, 30min) the larger sample count of RR leads to an improvement compared to NEE. FNEE outperformes RR and NEE in both cases.

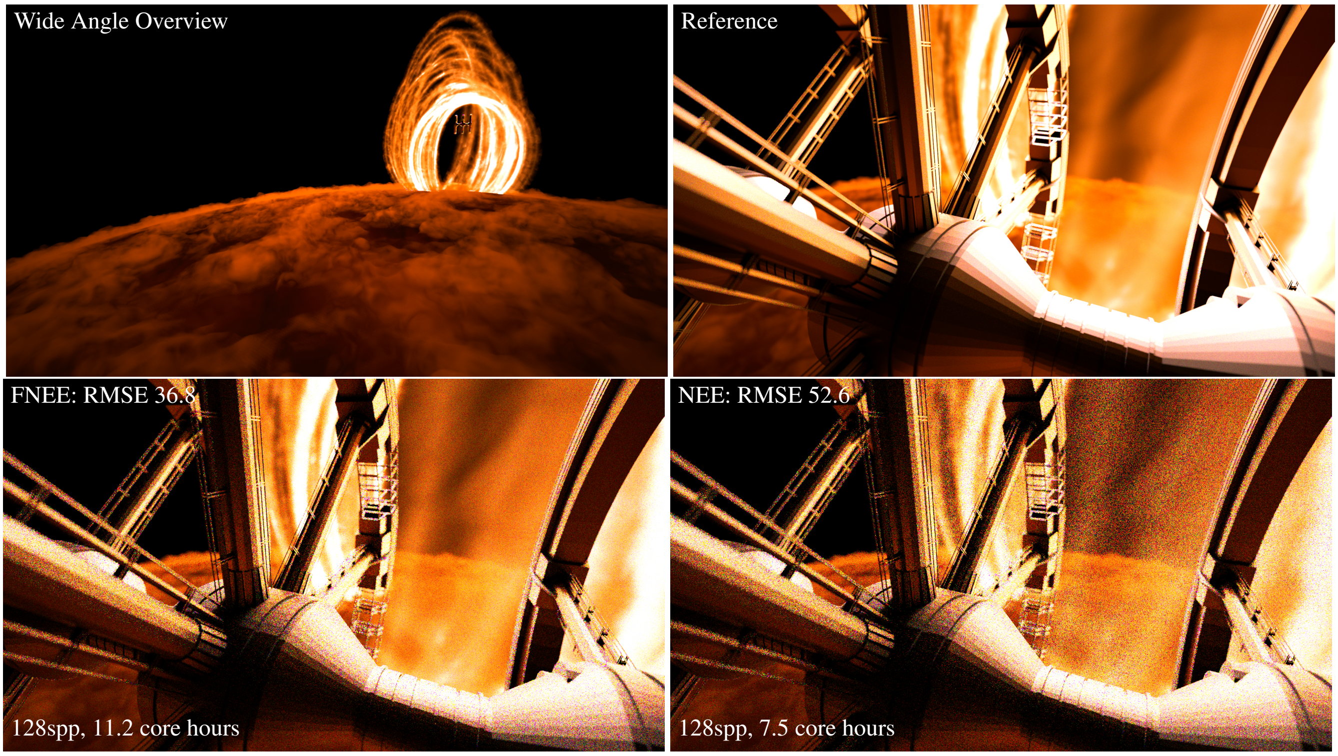

Figure 4: *Scalability test on a 30GB volume. These images show equal sample counts, the time is given in core hours, i.e. the time one core would need to create the image. Most of the light comes from the relatively thin loop – a case which works reasonably well with regular NEE. Note that this is a difficult scenario for FNEE as it creates long segments through the thin medium, i.e. it has a higher cost per sample than NEE. However, this is still amortized by collecting the emission along the path segment: the RMSEs for equal-time (60 core hours) are 14.9 FNEE (704spp) and 18.6 NEE (1024spp), respectively.*